Convergence and sampling efficiency in replica exchange simulations of peptide folding in explicit solvent

Xavier Periole and Alan E. Mark

Convergence and sampling efficiency in replica exchange simulations of peptide folding in explicit solvent

Xavier Periole[a)]

Department of Biophysical Chemistry, Groningen Biomolecular Sciences and Biotechnology Institute (GBB), University of Groningen, Nijenborgh 4, 9747 AG Groningen, The Netherlands

Alan E. Mark

Department of Biophysical Chemistry, Groningen Biomolecular Sciences and Biotechnology Institute (GBB), University of Groningen, Nijenborgh 4, 9747 AG Groningen, The Netherlands; School of Molecular and Microbial Sciences, St. Lucia 4072, Queensland, Australia; and the Institute of Molecular Biosciences, University of Queensland, St. Lucia 4072, Queensland, Australia

Replica exchange methods (REMs) are increasingly used to improve sampling in molecular dynamics (MD) simulations of biomolecular systems. However, despite having been shown to be very effective on model systems, the application of REM in complex systems such as for the simulation of protein and peptide folding in explicit solvent has not been objectively tested in detail. Here we present a comparison of conventional MD and temperature replica exchange MD (T-REMD) simulations of a β-heptapeptide in explicit solvent. This system has previously been shown to undergo reversible folding on the time scales accessible to MD simulation and thus allows a direct one-to-one comparison of efficiency. The primary properties compared are the free energy of folding and the relative populations of different conformers as a function of temperature. It is found that to achieve a similar degree of precision T-REMD simulations starting from a random set of initial configurations were approximately an order of magnitude more computationally efficient than a single 800 ns conventional MD simulation for this system at the lowest temperature investigated (275 K). However, whereas it was found that T-REMD simulations are more than four times more efficient than multiple independent MD simulations at one temperature (300 K) the actual increase in conformation sampling was only twofold. The overall gain in efficiency using REMD resulted primarily from the ordering of different conformational states over temperature, as opposed to a large increase of conformational sampling. It is also shown that in this system exchanges are accepted primarily based on (random) fluctuations within the solvent and are not strongly correlated with the instantaneous peptide conformation raising questions in regard to the efficiency of T-REMD in larger systems. © *2007 American Institute of Physics.*
[DOI: 10.1063/1.2404954]

INTRODUCTION

In the early 1960s Anfinsen *et al.* first showed that the sequence of a protein contains all the information needed for it to adopt its native fold.[1] Since then the challenge from both experimental and theoretical perspectives has been to identify the nature of the forces that drive protein folding.[2] Experimentally the primary challenge when characterizing protein folding in atomic detail is the speed of the structural transitions in comparison with the time resolution of the biophysical techniques currently available that can be used to provide structural information on single molecules. In contrast, for atomistic molecular dynamics (MD) simulations, the predominant theoretical approach used to model protein folding, the challenge is that structural transitions in proteins are rare and that it is simply not possible to explore sufficient conformational space (CS) on the time scales currently accessible. This inability to sample phase space currently limits simulations of folding using conventional MD to systems of approximately 10–20 residues.[3]

The most common approach to increase sampling is to reduce the computational cost of the simulation, for example, by reducing the number of degrees of freedom of the system and/or decreasing the complexity (and accuracy) of the force field such as by the use of lattice models[4,5] and implicit solvents models.[6] Alternatively, one can use strategies that allow the system to explore regions of the conformational space otherwise inaccessible. These range from simple simulated annealing[7] to more sophisticated methodologies such as adaptive umbrella sampling[8] or self-guided approaches[9–11] (see Refs. 12 and 13 for review). One recently developed technique that has shown considerable promise is the replica exchange method (REM). Temperature based REM (T-REM) combines simulated tempering and multicopy simulations in a thermodynamic correct manner.[14–16] Using T-REM, N independent copies (replicas) of the systems are propagated simultaneously at different fixed temperatures. At regular in-

---
[a)]Author to whom correspondence should be addressed. Tel.: +31-503634329. Fax: +31-503634398. Electronic mail: x.periole@rug.nl

tervals pairs of replicas at successive temperatures are exchanged according to a Metropolis criterion allowing individual replicas to sample a range of temperatures. At higher temperatures the increased thermal energy facilitates the exploration of conformational space and allows the system to cross barriers not readily crossed at the temperature of interest on a given time scale. T-REM has been shown to be very effective in enhancing conformational sampling in model systems.[14,15,17–19] However, although widely used[12,13,16,20,21] there has been only limited objective testing of T-REM in larger, more complex systems. In particular, the effectiveness of T-REM when simulating peptide or protein folding in explicit solvent where the solvent-solvent interaction dominates the total potential energy of the system is uncertain.

Rao and Caflisch[19] compared temperature replica exchange MD (T-REMD) and MD simulations of a 20-residue peptide in implicit solvent and concluded that both approaches produce similar energetic and structural properties of the peptide. Although the authors performed relatively long MD simulations (several microseconds) the exploration of the accessible CS at low temperature was extremely limited and the authors could not directly address the question of computational efficiency. More recently a similar study was performed on a 21-residue peptide, the Fs-21, also in implicit solvent.[18] By comparing the correlation times of the peptide helicity the authors found that T-REMD was between 14 and 72 times (decreasing with temperature) more efficient in regard to the sampling of CS than conventional MD simulations. The authors also noted the difficulties associated with the slow convergence of both the MD and T-REMD simulations at low temperature. When using an implicit representation of the solvent it is clear that the potential energy of the system will directly reflect the conformation of the peptide. However, a number of studies have demonstrated the need to use an explicit representation of the solvent to generate accurate free energy landscapes.[22–25] In particular, in their pioneering works on T-REMD simulations Zhou,[23] Zhou and Berne,[24] and Nymeyer and Garcia[25] showed that even if the native state was a local minimum in the free energy surface using an implicit solvent model it was not necessarily the global minimum and there were significant differences in the nature of the unfolded states. In particular, the unfolded conformations were found more extended in implicit solvent.[25] The difficulty is that in explicit solvent simulations the total potential energy of the systems is dominated by the solvent-solvent interaction and is not solely determined by the conformation of the peptide. Nevertheless, Sanbonmatsu and Garcia[26] observed a fivefold enhancement in sampling using T-REMD (16 replicas×2 ns per replica) compared with the equal amount of simulation time (32 ns) using conventional MD for the pentapeptide Met-enkephalin in explicit solvent. Although the system simulated was small, few structural transitions were observed in MD and full convergence could not be obtained using conventional MD nor was it conclusively demonstrated in the T-REMD simulations.

Here we present a detailed comparison of conventional MD and T-REMD of a β-heptapeptide in explicit solvent. This system is one of the very few for which a direct comparison between MD and T-REMD simulations of reversible peptide folding in explicit solvent can be performed. It has been previously shown that this peptide reversibly folds on a 10–100 ns time scale in MD simulations.[27,28] In this work we examine in detail a range of different factors effecting T-REMD simulations. We directly compare the rate of convergence and the computational efficiency of such simulations to standard MD simulations and consider whether the T-REMD simulations in practice yield the same thermodynamic properties and conformational sampling as standard MD in explicit solvent. We also compare T-REMD simulations to multiple independent MD simulations run at one temperature.

METHODS

The system

The system used in this study consisted of a β-heptapeptide [H-β-HVal-β-HAla-β-HLeu-(S,S)-β-HAla(αMe)-β-HVal-β-HAla-β-HLeu-OH] in methanol. This peptide has been shown previously to reversibly fold on a 10–100 ns time scale in simulations using the GROMOS force-field 43a1 (Refs. 27 and 28) and to accurately reproduce the folded structure as determined experimentally by NMR.[29] All simulations [MD and T-REMD] were performed using the GROMACS 3.1 package.[30,31] The peptide and solvent were described using the GROMOS force-field 43al (Ref. 32) as implemented in the GROMACS package. The peptide was solvated in 988 molecules of methanol in a cubic box (edge=39.60 Å). In all simulations the peptide and the solvent were, independently, weakly coupled to the desired temperature with a relaxation time of τ_T=0.1 ps.[33] Simulations were performed at both constant pressure (NPT) and constant volume (NVT). When pressure coupling was used the pressure was weakly coupled to 1 atm with a relaxation time of τ_P=1 ps.[33] Otherwise the volume was fixed to the volume of the system equilibrated at 300 K and 1 atm. A twin-range cutoff (1.0–1.4 nm) was used for the nonbonded interactions. Interactions within the short-range cutoff were evaluated every time step whereas interactions within the longer-range cutoff were evaluated every ten steps together with the pair list. To correct for the truncation of electrostatic interactions beyond the long-range cutoff a reaction-field correction was applied.[34]

Conventional molecular dynamics (MD)

MD simulations were performed in both NPT and NVT ensembles. The system was simulated at six temperatures (275.3, 286, 298, 322, 348, and 399 K) covering the range of temperature used in the REMD. All simulations were started from the same conformation, the NMR model equilibrated for 1 ns at 300 K and 1 atm. The backbone root mean square positional deviation (rmsd) of this conformation from the NMR model was 0.24 nm (residues 2–6). The system was simulated for 200 ns at 348 and 399 K, 400 ns at 322 K, and for 800 ns at 275.3, 286, and 298 K (see Table I). The system was also simulated 20 times for 20 ns at 300 K in the NVT ensemble. The 20 different starting structures were randomly selected from a simulation at 400 K. They were the

TABLE I. A summary of the simulations performed. Random: starting structures randomly selected from a simulation at 400 K. REMD-eq: starting structures taken from an equilibrated distribution (REMD-0.5 after 10 ns). REMDinv: inverted velocity scaling (see text).

	REMD		
Label	Starting structure	Exchange interval (ps)	Length (ns)
REMD-0.5	Random	0.5	20
REMD-2.0	Random	2.0	20
REMD-5.0	Random	5.0	20
REMDinv-0.5	Random	0.5	10
REMDinv-5.0	Random	5.0	10
REMDeq-0.1	REMD-eq	0.1	10
REMDeq-0.5	REMD-eq	0.5	10
REMDeq-2.0	REMD-eq	2.0	10
REMDeq-5.0	REMD-eq	5.0	10

	MD		
		Length (ns)	
Label	Temperature (K) $X=$	NPT	NVT
MD-X-275	275.3	800	800
MD-X-287	286.8	800	800
MD-X-298	297.8	800	800
MD-X-322	322.1	400	400
MD-X-348	348.4	200	200
MD-X-400	399.6	200	200
20-MDs	300.0	⋯	20×20

same as those used for the T-REMD simulations (see below). Conformations were saved every 10 ps for analysis.

Temperature replica exchange molecular dynamics (T-REMD)

The T-REMD methodology as derived by Sugita and Okamoto[15] has been described in detail elsewhere.[16,35,36] In brief, a given number of alternate starting conformations of a system (replicas) are independently propagated at different temperatures simultaneously. At regular intervals pairs of replicas are exchanged according to a Metropolis criterion,[15] which gives a probability of exchange between two replicas i and j: $P(i,j) = \exp[-(\beta i - \beta j)(Ej - Ei)]$, where $\beta = 1/k_B T$, E is the potential energy of the system, T the absolute temperature, and k_B Boltzmann's constant. By allowing replicas to explore temperature space, T-REMD allows the system to cross energetic barriers and thus access regions of the CS difficult to reach at low temperatures. In order to ensure a uniform exchange probability the temperatures were chosen according to the relation: $T_i = T_0 \exp(ic)$, proposed by Sugita and Okamoto,[15] where T_0 and c can be varied to give the desired exchange ratio. Using $T_0 = 270$ K and $c = 0.0196$ 20 temperatures were generated: 275.3, 280.8, 286.4, 292.0, 297.8, 303.7, 309.7, 315.8, 322.1, 328.5, 335.0, 341.6, 348.4, 355.3, 362.3, 369.5, 376.8, 384.2, 391.8, and 399.6 K. In order to investigate the effect of exchange frequency and possible correlations between exchanges the time interval between two exchange trials was varied between 0.1, 0.5, 2.0,

and 5.0 ps. To ensure a smooth transition of the system from one temperature to another and that there is no net exchange of energy between the replicas the velocities of the particles in the system must be scaled by $(T_{final}/T_{init})^{1/2}$. If not done successive exchanges may be correlated (i.e., have a high probability of back exchange).

The setup of the T-REMD simulations was identical to that of the MD simulations in the NVT ensemble. For the simulations REMD-0.5, REMD-2.0, and REMD-5.0 the 20 starting structures were extracted from the first 40 ns of a simulation at 400 K (MD-NVT-400) (see Table I). The structures were selected such that the backbone rmsd from the experimental NMR structure was >0.3 nm. In addition individual structures were separated by more than 1 ns in the trajectory to ensure that they were not correlated. Simulations REMDeq-0.1, REMDeq-0.5, REMDeq-2.0, and REMDeq-5.0 were initiated from REMD-0.5 at 10 ns at which point the system is fully equilibrated. All simulations performed in this study are summarized in Table I.

Population analysis and clustering

To determine the probability of the peptide adopting specific conformations during the simulations the trajectories were clustered using the method of Daura et al.[28] First, a matrix of positional rmsd between all conformations was constructed. The conformation with the most neighbors within a specified cutoff was then determined. This structure (the center or representative configuration of the first cluster), together with all of its neighbors, were then removed from the ensemble and the procedure repeated to obtain the second and higher clusters until the set of structures was empty. In this work, two conformations were considered neighbors if their rmsd was <0.07 nm. This distance corresponded to the first minimum in the histogram of the complete positional rmsd matrix of the backbone atoms (residues 2–6) calculated from the simulation MD-NPT-275 (data not shown) that showed a good separation of the different populations.

Folding free energy

The free energy of folding was calculated from the ratio of folded to unfolded conformations as $\Delta G^T = -RT \log(P_{fold}^T / P_{unfold}^T)$, where P_{fold}^T and P_{unfold}^T are the probabilities of the peptide being folded and unfolded, respectively, at the temperature T. P_{unfold}^T was estimated as $1 - P_{fold}^T$. P_{fold}^T was taken as the ratio of structures that have a positional rmsd (backbone atoms of residues 2–6) from the NMR model[29] lower than a cutoff of 0.07 nm, which corresponds to the first minimum of the distribution of the positional rmsd from the NMR model for simulation MD-NPT-275 and defines the separation between folded and unfolded peptides.

RESULTS AND DISCUSSION

The results and discussion are organized as follows. First, an analysis of the reference MD simulations is presented followed by an analysis of factors affecting the T-REMD simulations. Finally, a comparison between the
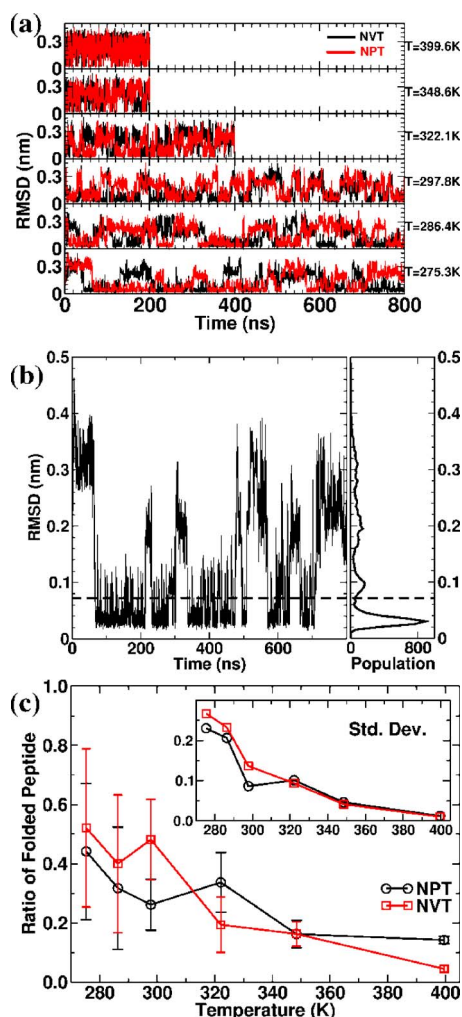
FIG. 1. (Color online) MD simulations. (a) Time evolution of the positional rmsd (backbone atoms of residues 2–6) with respect to the experimental NMR structure for MD-*NVT* (black) and MD-*NPT* (red) simulations at different temperatures. (b) Time evolution of the positional rmsd (backbone atoms of residues 2–6) for MD-*NPT*-275 together with a histogram of rmsd value (right) distribution. The dashed line shows the separation between folded and unfolded basins (rmsd=0.07 nm). (c) Ratio or fraction of folded conformations, P_{fold}^{T}, sampled as a function of the temperature, the inset contains one standard deviation (std. dev.).

MD and T-REMD simulations is presented in terms of the folding free energy, the sampling of the conformational space, and the computational cost.

MD reference simulations

The β-heptapeptide was simulated at six different temperatures (275.3, 286, 298, 322, 348, and 399 K) spanning the range of temperature used for the T-REMD simulations (see Methods). Figure 1(a) shows a time series of the backbone rmsd (residues 2–6) of the peptide from the NMR model[29] at the different temperatures for trajectories in the *NVT* (black line) and *NPT* (red line) ensembles. In all cases the peptide is observed to undergo multiple folding and unfolding transitions as indicated by the rmsd jumping from low (∼0.03 nm) to high (∼0.25 nm) values. As expected the frequency of those transitions increases with the temperature.

Figure 1(b) shows the time series of the positional rmsd of the backbone atoms (residues 2–6) for MD-*NPT*-275 in

more detail together with a histogram of the corresponding rmsd values. The first and largest peak corresponds to the set of structures that can be considered fully folded with an average positional rmsd of 0.03 nm from the experimentally determined NMR model.[29] The remaining structures are considered unfolded for the purpose of this work. The minimum between the first and second peaks indicated by the dashed line in Fig. 1(b) (rmsd=0.07 nm) marks the separation between the folded and unfolded states.

The ratio of the folded peptide to the total conformations as a function of the temperature is plotted in Fig. 1(c) for both the MD-*NVT* and MD-*NPT* simulations. The error bars correspond to one standard deviation calculated using windows of 100 ns. The decrease in standard deviation as a function of temperature [inset of Fig. 1(c)] primarily reflects improved statistics at high temperature associated with the increased number of transitions. Standard errors would be more appropriate for the present analysis, but the trend would not be affected. The ratio of folded to unfolded peptide as a function of temperature is similar in the *NPT* and the *NVT* ensembles especially at low temperature. Nevertheless, even at 298 K where the MD-*NVT* and MD-*NPT* simulations are essentially identical significant differences are evident. The discrepancy results from a high ratio of folded peptide (∼60%) in the first half of the MD-*NVT*-298 simulation. This indicates that even after 800 ns the simulations are not fully converged. It is only at 400 K where the simulations are well converged that it is possible to unequivocally detect differences between the simulations performed in the two ensembles with the constant volume (high pressure) simulation favoring the unfolded state of the peptide.

REMD simulations
Exchange ratio

The acceptance ratio between two temperatures is determined from the overlap of their respective potential energy distributions. To maintain a constant acceptance ratio the spacing between target temperatures in a T-REMD simulation must increase with the temperature. In this work the exponential distribution suggested by Sugita and Okamoto[15] was used. That the temperature spacing does give a constant acceptance ratio is shown in Fig. 2(a). A critical parameter determining the efficiency of T-REMD simulations is the interval between exchanges. Ideally the acceptance ratio should be independent of the interval between successive exchange trials. As can be seen in Fig. 2(a) while the acceptance ratio for intervals of 0.5, 2.0, and 5.0 ps was on average 0.27, it increased to 0.30 for an exchange interval of 0.1 ps suggesting that below 0.5 ps consecutive exchanges were correlated.

To investigate the correlation in the system further, *direct exchanges* were distinguished from *random exchanges*. By direct exchanges we refer to exchanges in which the potential energy of the system at the higher temperature was lower than that of the system at the lower temperature. Such exchanges are always accepted. By random exchanges we refer to cases in which although the potential energy of the system at higher temperature was higher than that at lower
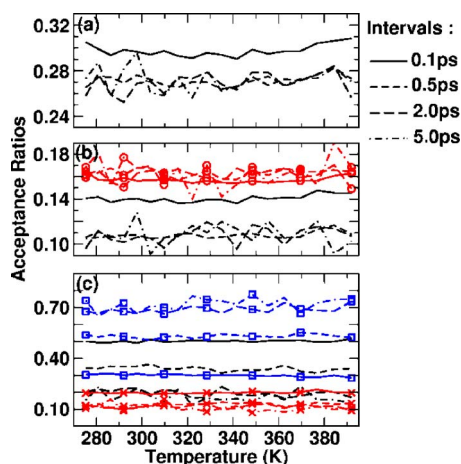
FIG. 2. (Color online) Acceptance ratio for trial exchanges between consecutive temperatures. (a) Global acceptance ratio. (b) A decomposition of the total number of exchanges into direct (black) and random (red; circles) exchanges. (c) Percentage of the direct exchanges that occur (i) following a random exchange (back exchange) (black; no symbol), (ii) following a direct exchange (red; crosses), and (iii) following a rejected exchange (blue; squares).

temperature an exchange was accepted after comparing the probability of finding this combination of state to a random variable as part of the Metropolis test. As can be seen in Fig. 2(b), the probability of a random exchange following a given trial for this system is 0.16 and that, to a first approximation, this is independent of the interval between exchange trials. Random exchanges represent about 60% of the total number of accepted exchanges. The probability of a direct exchange is approximately 0.11 for intervals of 0.5 ps and greater but is 0.14 with an interval of 0.1 ps.

Direct exchanges are further separated in Fig. 2(c) which shows the percentage of direct exchanges that occur immediately following a random exchange or back exchange (black; no symbol), the percentage that occur immediately following a direct exchange (red; crosses), and the percentage immediately following a failed exchange (blue; squares). The three types of direct exchange occur with a similar probability for intervals of 2.0 and 5.0 ps, indicating that there is no correlation between exchange trials. Deviations are, however, observed for intervals of 0.1 and 0.5 ps. As can be seen in Fig. 2(c) there is a large progressive increase in the probability of immediate back exchange (following a random exchange) from ∼0.20 for an interval of 2.0 or 5.0 ps to ∼0.32 for an interval of 0.5 ps and to ∼0.50 for an interval of 0.1 ps. This indicates that successive configurations using an interval of 0.5 ps but especially using an interval of 0.1 ps are strongly correlated. Interestingly, using an interval of 0.5 ps, the increase in back exchanges is largely compensated by a decrease in exchanges following a failed trial meaning that the overall probability of a direct exchange using an interval of 0.5 ps does not differ significantly from that using 2.0 or 5.0 ps. Note that the probability of back exchange is higher immediately after a random exchange as the potential energy difference between the two configurations is inverted. Thus, if there is no change in the relative potential energy the back exchange will always be accepted. The fact that the correlation times are so short is surprising

and indicates that small local structural variations that occur on a 0.5–2.0 ps time scale dominate the exchange probability as opposed to larger scale motions.

Although the effect of a too short exchange interval on the probability of back exchanges is relatively large, as back exchanges simply return the system to its original state, their effect on the overall efficiency of the approach is limited. This is evident in the case of an interval of 0.5 ps where the rate of back exchange is increased but the overall rate of exchange is largely unaffected.

In order to investigate the effective correlation times in this system further a series of simulations was performed in which the scaling of the velocities following an exchange was inverted $[(T_{init}/T_{final})^{1/2}]$. This enhances the probability of finding the state at the higher temperature at lower energy and increases the degree of correlation after exchanges. Nevertheless, while effects were again seen using intervals of 0.1 and 0.5 ps no effect was observed using intervals of 2.0 and 5.0 ps (results not shown). This demonstrates that velocity scaling while formally required is in practice of minor importance.

Potential energy distribution

Figure 3 shows the distribution of the total potential energy of the system [Fig. 3(a)] and the peptide [Fig. 3(b)] as a function of temperature for REMD-0.5. Although the distribution of the total potential energy follows the expected distribution for T-REMD simulation,[26] the distribution of the potential energy of the peptide does not [Fig. 3(b)]. There is a clear effect of temperature, but the distributions are far from Gaussian. There is a high degree of overlap between the potential energy distributions and if the potential energy of the peptide was used to determine the exchanges one would expect the acceptance ratio to be close to 50%, the value for two overlapping distributions. However, the potential energy of the peptide represents only 1% of the total potential energy. The contribution of the peptide to variations in the total potential energy is <0.5%. Even if the interaction of the peptide with the solvent is included, these values do not vary significantly with the contribution to the total potential energy rising to just 3%. The potential energy distributions are similar to those shown in Fig. 3(b). Clearly, specific exchanges are primarily determined by fluctuations in the solvent-solvent interactions, not changes in the potential energy of the peptide. This accounts for the short correlation time described above. However, averaged over many exchanges the system is sensitive to the conformation of the peptide as is evidenced from the convergence in the populations at specific temperatures.

Temperature exploration

The average residence times between successive temperature jumps were found to be 1.7, 7.4, and 18.5 ps for intervals between exchange trials of 0.5, 2.0, and 5.0 ps, respectively. Thus, to a first approximation the frequency of temperature jumps was directly proportional to interval between exchange trials. This is also reflected in the manner in which two replicas explore the full temperature range as a
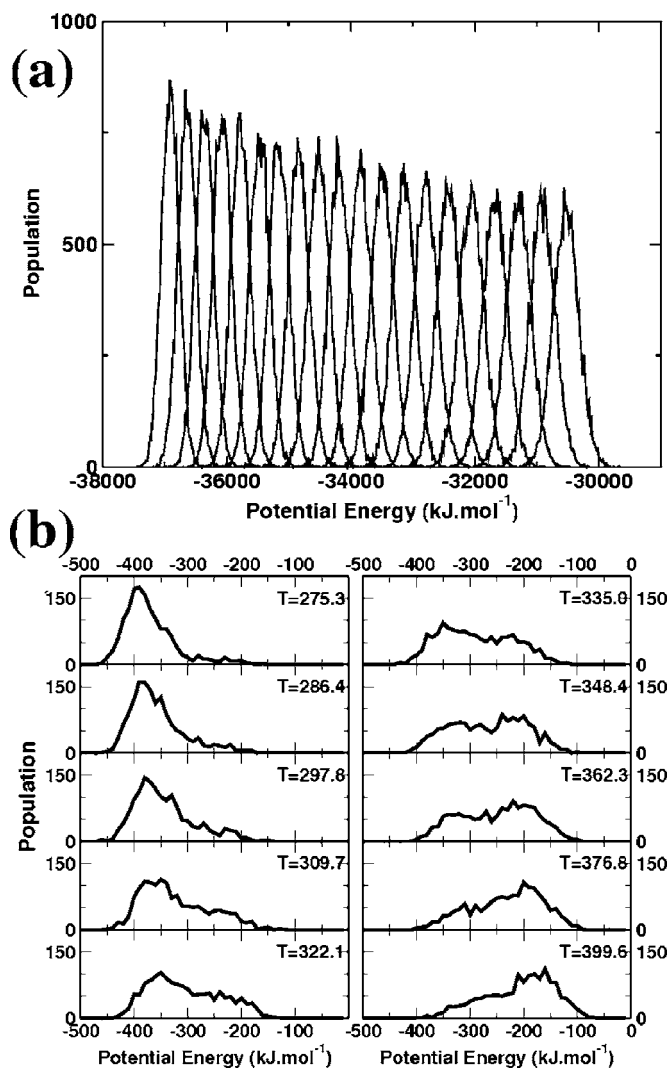

ation

ishing

.

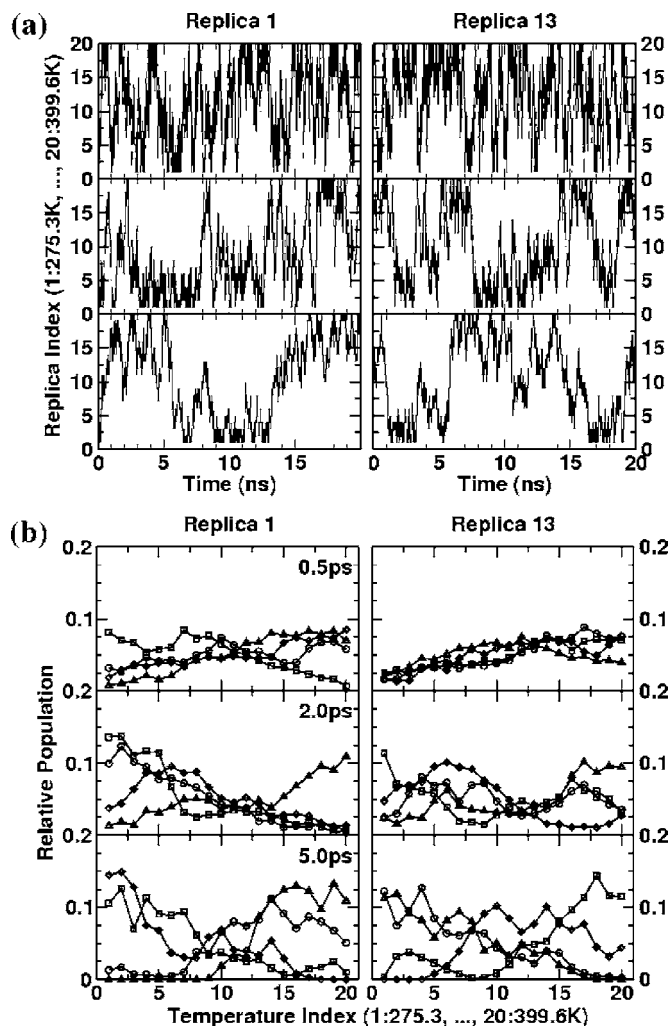FIG. 3. Potential energy distributions for (a) the total system and (b) the peptide.

FIG. 4. Examples of how individual replicas sample temperature space. (a) The effect of increasing the interval between exchange trials (0.5, 2.0, and 5.0 ps; top to bottom) for replicas 1 and 13. (b) The relative populations (time spent) of replicas 1 and 13 at a given temperature average of separate 5 ns windows for the different intervals between exchange trials.

function of the interval between exchange trials as illustrated in Fig. 4(a). A smaller interval between trials results in more frequent transitions between temperatures and a more even sampling of temperature. This is true despite the fact that the apparent residence time in a given range of temperatures, which from Fig. 4(a) can be seen to be on the nanosecond time scale, is very much longer than the interval between trial exchanges. Figure 4(b) shows the relative amount of time a specific replica spends at a given temperature averaged over separate 5 ns windows. As can be seen the distributions are largely converged after 5 ns using an interval of 0.5 ps between exchanges but not when longer intervals are used.

RMSD and ratio of folded peptide

The time series of the backbone rmsd (residues 2–6) of the peptides from the NMR model[29] in the simulations REMD-0.5, −2.0, and −5.0 at ten different temperatures are shown in Fig. 5. Many transitions between low and high rmsd values are observed. Note that these transitions primarily correspond to exchanges between replicas at different temperatures as opposed to the folding or unfolding of an

individual peptide at a given temperature although the latter does also occur. As the residence time of a replica at a given temperature is directly proportional to the frequency of trial exchanges the apparent number of transitions increases as the interval between exchanges is decreased.

As expected the peptide has a higher propensity to be folded at lower temperature. This is most apparent in the simulation REMD-5.0. To determine the ratio of folded peptide the same criterion as used previously for the reference MD simulations was applied. The results calculated using the last 15 ns of the simulations REMD-0.5, REMD-2.0, and REMD-5.0 are plotted in Fig. 6(a). The error bars again correspond to one standard deviation calculated using three windows of 5 ns (the first 5 ns were discarded). The results from the three simulations are similar over the full range of temperature. They are effectively identical above 350 K and lie within one standard deviation of each other below 350 K. In addition the standard deviation of the results is roughly similar in each of the simulations [see inset of Fig. 6(a)] indicating that the simulations have reached an equivalent degree of precision.
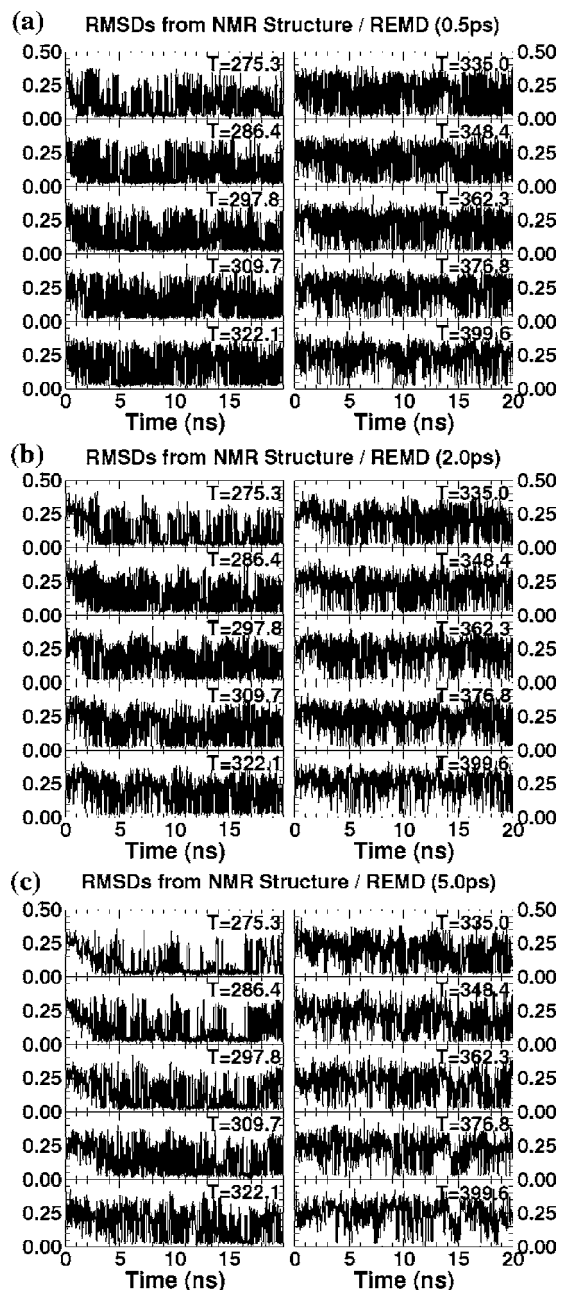
FIG. 5. Positional rmsd from the NMR model for REMD-0.5 (top panel), REMD-2.0 (middle panel), and REMD-5.0 (bottom panel). Note that results for only 10 of the 20 temperatures are plotted.

FIG. 6. (Color online) The ratio of folded peptide (P_{fold}^T) for the REMD simulations as a function of temperature. (a) Average ratio of folded peptide (P_{fold}^T) for the last 15 ns of the simulations for different exchange intervals (black circles, 0.5 ps; red diamonds, 2.0 ps; green crosses, 5.0 ps). The error bars correspond to one standard deviation from the mean (std. dev.). The inset shows the change in std. dev. as a function of temperature. (b) The ratio of folded peptide (P_{fold}^T) for different time windows. The black line corresponds to average after equilibration (6–20 ns). The error is given as two std. devs. from the mean. The red (circles), green (diamonds), and blue (crosses) lines correspond to averages over the periods of 0–2, 2–4, and 4–6 ns, respectively.

Efficiency and the interval between exchange trials

The relative efficiency of the T-REMD simulations was estimated from the time needed to reach equilibrium in terms of the ratio of folded peptide at the temperature of interest. Figure 6(b) shows the ratio of folded peptide calculated over different time intervals: 0–2, 2–4, 4–6, and 6–20 ns. From this it can be seen that there is an initial latent period that depends on the interval between exchange trials. At T =275 K this latent period is approximately 1–2 ns for an interval of 0.5 ps, is 2–3 ns for an interval of 2.0 ps, and is 3–4 ns for an interval of 5.0 ps. This period can be equated to an equilibration time in the sense that replicas have first to fold and second to distribute over the range of temperatures. For the current case 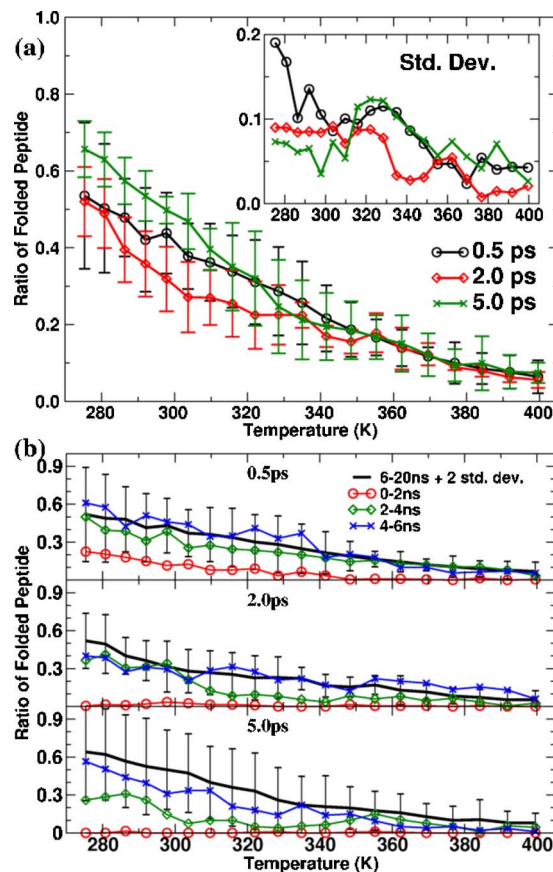it is clear that the efficiency of the meth-odology increases as the frequency of exchanges increases (i.e., as the intervals between exchange trials decrease). This is until the successive exchanges become correlated ($\leq$0.5 ps). Note that this latent period will depend on the initial set of conformations. In this case the peptide simulated folds very rapidly in comparison with the length of the simulations and thus the effect of the initial conformation on convergence is expected to be small. Other than this initial latent period no significant effect of the interval between the exchange trials on the overall rate of convergence was evident.

MD versus T-REMD
Folding free energy

Figure 7 shows the free energy of folding (see Methods) as a function of temperature for the simulations REMD-0.5, REMD-2.0, REMD-5.0, MD-*NVT*, and MD-*NPT*. As expected, the results are very similar except for the simulations performed under *NPT* conditions at high temperature. This
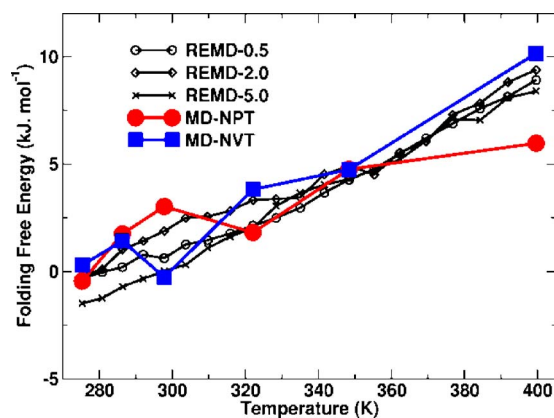
FIG. 7. (Color online) The free energy of folding calculated from the ratio of folded to unfolded peptide (see Methods) as a function of temperature obtained using different intervals between exchanges and for conventional MD in the *NVT* and *NPT* ensembles.
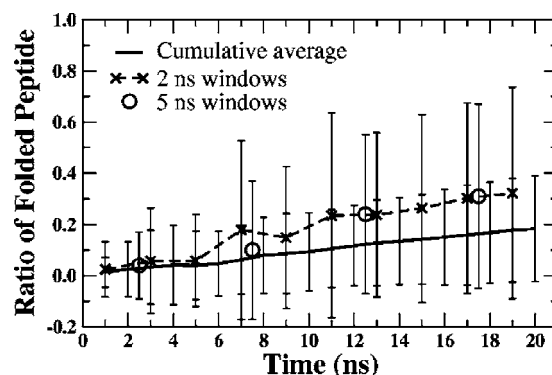

FIG. 8. The average ratio of folded peptide (P_{fold}^{T}) for 20 independent MD simulations started from random configurations at 300 K. The black line corresponds to the time cumulative average, the dashed line (crosses) to values obtained for consecutive 2 ns windows, and the circles to values obtained for consecutive 5 ns windows. The error bars represent one std. dev. from the mean of the 20 simulations.

suggests that the T-REMD simulations yield the same thermodynamic properties as the MD simulations.

Sampling of conformational space

To determine whether the different protocols sampled the same regions of conformational space the four most populated clusters, together with their representative structure, were extracted from the MD-*NVT*, MD-*NPT*, and REMD-0.5 simulations at *T*=275, 286, 298, 322, 348, and 399 K. The clusters were obtained from the full trajectory of the MD simulations and the last 15 ns of REMD-0.5. The relative populations of the 72 resulting clusters are given in Table II. In all simulations one cluster dominates. The following three clusters in general each represent <10% of the total population.

To evaluate the similarity of the clusters obtained using the three protocols at different temperatures the central or representative structure from each of the 72 clusters was compared. Structures with a backbone rmsd <0.04 nm are indicated in Table II. Five conformations were unique (underlined). As can be seen from Table II, even at the highest temperatures the ensemble is dominated by the same four conformations and that the folded structure at 273 K, which corresponds to the NMR model,[29] dominates at all temperatures. The results in Table II also show that within the error MD and T-REMD generate the same populations at all temperatures.

Computational efficiency

To estimate the relative cost and computational efficiency of the MD and T-REMD simulations a comparison has been made based on the minimal time required to obtain a specific degree of precision over a range of temperatures. In the case of conventional MD the full simulation length was used. As shown in Fig. 1(c), at low temperatures (275.3, 286.8, and 292.8 K) even after 800 ns the populations have not fully converged. For T-REMD the most efficient protocol used a 0.5 ps interval between exchange trials (REMD-0.5). For this protocol it was found that 2 ns was sufficient for the system to initially relax [Fig. 6(b)], and a further 2–3 ns was required to give sufficient sampling to obtain apparently converged populations at all temperatures equivalent to that obtained using conventional MD. Thus, 5 ns of T-REMD was required in total. For determining the relative populations at the lower temperatures (275–300 K), T-REMD was at least eight times more efficient than conventional MD for this system (20×5 ns compared with 800 ns). However, if the full melting curve was to be determined as shown in Fig. 7 the T-REMD would be approximately 30–50 times more efficient. Note that the difference in efficiency decreases at higher temperatures, whereas 800 ns was required to obtain convergence at 275–300 K using conventional MD only 200 ns or less is required at 400 K.

There is also the question of whether an *M* replica T-REMD simulation is more efficient than *M* individual MD

TABLE II. Cluster analysis of MD-*NPT*, MD-*NVT*, and REMD-0.5 (REMD). For each simulation the population (percentage of total number of configurations) of the first four clusters is indicated. The style (bold, regular, italic/bold, and italic/underlined) indicates central or representative structures of clusters with a backbone rmsd within 0.04 nm (residues 2–6). The style regular/underlined indicates unique conformations.

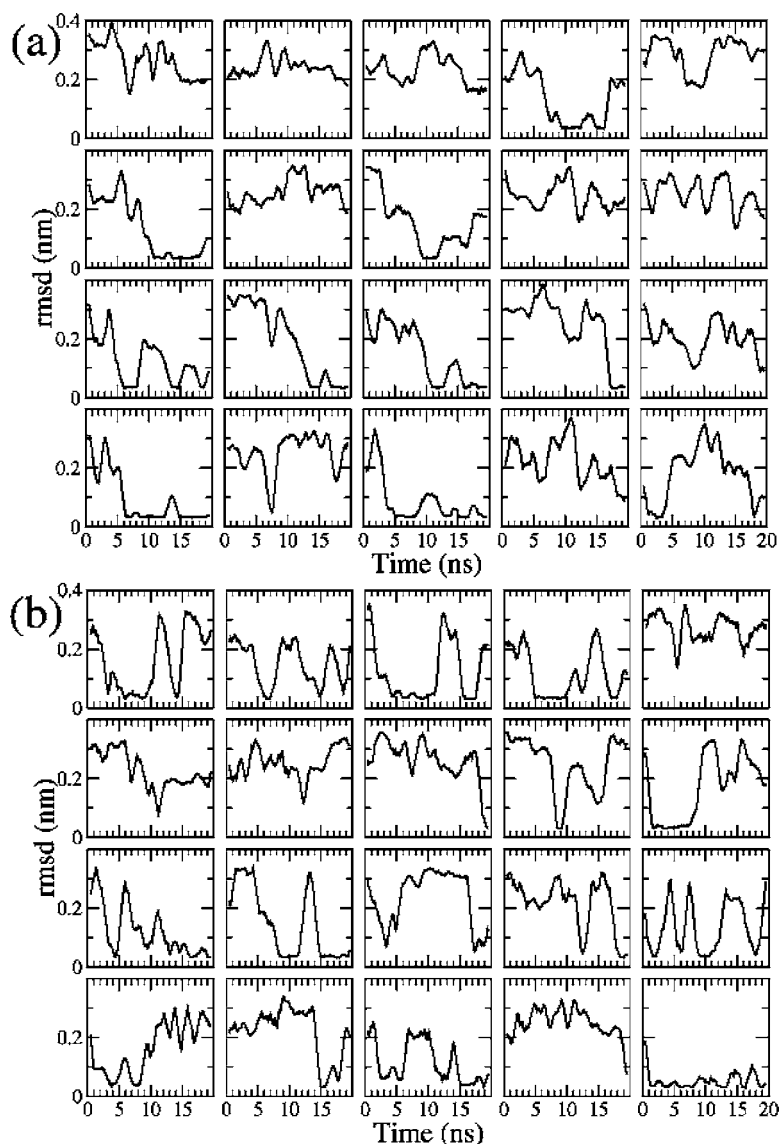| *T* (K)	275				286				298				322				348				400			
Cluster No.	1	2	3	4	1	2	3	4	1	2	3	4	1	2	3	4	1	2	3	4	1	2	3	4
MD-*NPT*	**50**	8	*5*	*3*	37	*10*	6	*4*	32	*7*	7	6	**38**	*6*	*5*	5	**18**	*10*	**4**	3	15	5	*4*	2
MD-*NVT*	**53**	*7*	*6*	5	46	11	6	*5*	**53**	7	*3*	*3*	21	6	*5*	*5*	19	*6*	5	**4**	5	*3*	2	*1*
REMD	**60**	*8*	7	*6*	54	*10*	6	*6*	51	6	*6*	5	35	*7*	6	4	22	*5*	*5*	**4**	8	3	*2*	2

FIG. 9. The rmsd from the NMR model for the 20 replicas simulated (a) by 20 independent MD simulations (b) in the REMD-0.5. The replica number goes from the left to the right and top to bottom.

simulations.[37] Figure 8 shows the ratio of folded peptide as a function of time averaged over 20 independent MD simulations starting from the same set of randomized initial configurations as used in the T-REMD simulations. As can be seen from Fig. 8 at 300 K, the set of simulations had not converged to the appropriate value of the ratio of folded peptide within the 5 ns simulation needed by a 20 replica T-REMD. Nevertheless, within 20 ns the ratio reached is within the range obtained in both the T-REMD and the extended conventional MD simulations. The fact that the results after 20 ns of simulation of each copy (total of 400 ns) are still dependent on the choice of initial conformation suggests two things: first that the set is not fully converged (a smaller set of simulations, each simulated longer might well be more efficient) second, that in the present case T-REMD is more effective (greater than four times at 300 K) than multiple MD simulations started from random conformations at a fixed temperature. Again the apparent efficiency will depend on initial set of configurations selected.

This leaves the question why REMD simulations are more efficient than conventional MD. Two factors contribute to the apparent increase in efficiency. The first is that at

higher temperatures potential energy barriers are more readily overcome meaning that replicas at higher temperature have increased conformational sampling. The second factor is that by having multiple replicas it is possible to sample a broad range of conformations and by allowing multiple exchanges approximate an ensemble at a given temperature. If one has a broad range of conformations but little sampling the fast mixing of the replicas can lead to apparent convergence and mask poor sampling. Rhee and Pande previously discussed this issue in their work on multiplexed REMD.[38] The quantification of these effects is not straightforward. In the current systems we have attempted to quantify the degree of sampling by counting the number of folding/unfolding events. In Fig. 9 the rmsd versus time is shown for 20 independent MD simulations and for the 20 replicas in REMD-0.5. A folding (unfolding) event was considered to occur if the rmsd from the NMR structure averaged over 1 ns windows crossed the folding/unfolding threshold of 0.07 nm. The number of folding/unfolding events is listed in Table III. From Table III it can be seen that for comparable simulations (the replica exchange and multiple simulations performed at 300 K started from the same initial configurations) the num-

TABLE III. Number of folding (*N*fold) and unfolding (*N*unfold) events counted in REMD-0.5, -2.0, -5.0, and 20 independent MD simulations. The counting was done on the running average (over 1 ns time periods) of the rmsd vs time (see Fig. 9) of equivalent time period of simulation (400 ns) and is expressed per 10 ns.

	REMD-*X*			
X=	0.5	2.0	5.0	20 MDs
*N*fold/*N*unfold	1.0/0.9	0.8/0.7	0.7/0.6	0.5/0.4

ber of folding/unfolding per 10 ns using the REMD protocol was only a factor of 2 larger than that obtained using multiple conventional MDs. Thus increased sampling due to certain replicas experiencing a higher temperature is not the primary factor leading to rapid equilibration of the populations in this case, but rather it is the rapid distribution or sorting of the conformation as a function of temperature. Nevertheless, the exchange frequency does play a role as the number of folding/unfolding events decreases with the time interval between exchange trials (Table III). The increase in sampling of temperature space does increase the extent of conformational sampling but only to a small extent. In summary, the effect of temperature on sampling efficiency in REMD simulations is small, whereas the effect of the distribution of conformers over different temperatures is large leading to high apparent efficiency for this system.

CONCLUSION

Temperature replica exchange molecular dynamics (T-REMD) and conventional molecular dynamics (MD) simulations of the reversible folding of a β-heptapeptide at equilibrium in explicit methanol have been compared. It has been shown that for the range of temperatures simulated (from 275 to 400 K) both approaches yielded similar melting curves (propensity of the peptide to be folded as a function of temperature) and similar population of the most abundant conformers. In terms of the total length of simulation required to reach comparable populations of the folded/unfolded states at a specific (lowest) temperature of interest T-REMD proved to be at least one order of magnitude more efficient than a single conventional MD simulation while at the same time providing converged distributions over the full range of temperatures. The T-REMD simulations were also shown to be more efficient than multiple independent MD simulations at one temperature (300 K). However, the conformational sampling in T-REMD when compared to multiple MDs was only increased by a factor of 2 suggesting that the increase in temperature has only a minor effect on the efficiency of REMD and that conformational sampling could place an upper limit on the efficiency of REMD. It is shown that the primary gain in efficiency comes from the mixing/sorting of the replicas over different temperatures. While this mixing/sorting can give rise to appropriate population distributions depending on the selection of initial configurations it can also give rise to false precision and be misinterpreted as true convergence or increased sampling efficiency.

The T-REMD simulations were shown to be most efficient when the intervals between exchange trials were chosen to be equal to the correlation time of the potential energy following an exchange. In the case of the β-heptapeptide in methanol the most efficient interval between exchanges was 0.5 ps. This suggests that the exchanges were primarily determined by fluctuations within the solvent rather than the conformation of the peptide. This raises questions in regard to the potential efficiency of the method for larger systems. We note in this regard that Seibert *et al.*[39] have recently shown that for an 11-residue peptide in water simulations on the order of 200 ns at each temperature were required to reach convergence in terms of the melting curve. Thus, although T-REMD is much more efficient that conventional MD simulations for rapidly equilibrating systems, such as the β-heptapeptide in methanol considered here, alternative protocols may be needed to fold larger systems.[40–43]

ACKNOWLEDGMENTS

[1] C. B. Anfinsen, E. Haber, M. Sela, and F. H. White, Jr., Proc. Natl. Acad. Sci. U.S.A. **47**, 1309 (1961).
[2] A. R. Dinner, A. Sali, L. J. Smith, C. M. Dobson, and M. Karplus, Trends Biochem. Sci. **25**, 331 (2000).
[3] L. Monticelli, D. P. Tieleman, and G. Colombo, J. Phys. Chem. B **109**, 20064 (2005).
[4] G. Trinquier and Y. H. Sanejouand, Phys. Rev. E **59**, 942 (1999).
[5] S. B. Ozkan, K. A. Dill, and I. Bahar, Protein Sci. **11**, 1958 (2002).
[6] T. Lazaridis and M. Karplus, Proteins **35**, 133 (1999).
[7] Y. Levy and O. M. Becker, J. Chem. Phys. **114**, 993 (2001).
[8] C. Bartels and M. Karplus, J. Comput. Chem. **18**, 1450 (1997).
[9] X. W. Wu and S. M. Wang, J. Chem. Phys. **110**, 9401 (1999).
[10] X. W. Wu and B. R. Brooks, Chem. Phys. Lett. **381**, 512 (2003).
[11] R. Bitetti-Putzer, A. R. Dinner, W. Yang, and M. Karplus, J. Chem. Phys. **124**, 174901 (2006).
[12] K. Tai, Biophys. Chem. **107**, 213 (2004).
[13] C. D. Snow, E. J. Sorin, Y. M. Rhee, and V. S. Pande, Annu. Rev. Biophys. Biomol. Struct. **34**, 43 (2005).
[14] U. H. E. Hansmann, Chem. Phys. Lett. **281**, 140 (1997).
[15] Y. Sugita and Y. Okamoto, Chem. Phys. Lett. **314**, 141 (1999).
[16] Y. Okamoto, J. Mol. Graphics Modell. **22**, 425 (2004).
[17] D. Bedrov and G. D. Smith, J. Chem. Phys. **115**, 1121 (2001).
[18] W. Zhang, C. Wu, and Y. Duan, J. Chem. Phys. **123**, 154105 (2005).
[19] F. Rao and A. Caflisch, J. Chem. Phys. **119**, 4035 (2003).
[20] D. J. Earl and M. W. Deem, Phys. Chem. Chem. Phys. **7**, 3910 (2005).
[21] A. Mitsutake, Y. Sugita, and Y. Okamoto, Biopolymers **60**, 96 (2001).
[22] X. Daura, A. E. Mark, and W. F. van Gunsteren, Comput. Phys. Commun. **123**, 97 (1999).
[23] R. H. Zhou, Proteins **53**, 148 (2003).
[24] R. H. Zhou and B. J. Berne, Proc. Natl. Acad. Sci. U.S.A. **99**, 12777 (2002).
[25] H. Nymeyer and A. E. Garcia, Proc. Natl. Acad. Sci. U.S.A. **100**, 13934 (2003).
[26] K. Y. Sanbonmatsu and A. E. Garcia, Proteins **46**, 225 (2002).
[27] X. Daura, B. Jaun, D. Seebach, W. F. van Gunsteren, and A. E. Mark, J. Mol. Biol. **280**, 925 (1998).
[28] X. Daura, W. F. van Gunsteren, and A. E. Mark, Proteins **34**, 269 (1999).

[29] D. Seebach, P. E. Ciceri, M. Overhand, B. Jaun, D. Rigo, L. Oberer, U. Hommel, R. Amstutz, and H. Widmer, Helv. Chim. Acta **79**, 2043 (1996).

[30] H. J. C. Berendsen, D. van der Spoel, and R. van Drunen, Comput. Phys. Commun. **91**, 43 (1995).

[31] E. Lindahl, B. Hess, and D. van der Spoel, J. Mol. Model. **7**, 306 (2001).

[32] W. F. van Gunsteren, S. R. Billeter, A. A. Eising, P. H. Hunenberger, P. Kruger, A. E. Mark, W. R. P. Scott, and I. G. Tironi, *Biomolecular Simulation: The GROMOS96 Manual and User Guide* (vdf Hochschulverag AG an der ETH, Zurich/Biomos BV, Groningen, 1996).

[33] H. J. C. Berendsen, J. P. M. Postma, W. F. van Gunsteren, A. Dinola, and J. R. Haak, J. Chem. Phys. **81**, 3684 (1984).

[34] I. G. Tironi, R. Sperb, P. E. Smith, and W. F. van Gunsteren, J. Chem. Phys. **102**, 5451 (1995).

[35] R. H. Zhou, Proc. Natl. Acad. Sci. U.S.A. **100**, 13280 (2003).

[36] A. E. Garcia and K. Y. Sanbonmatsu, Proteins **42**, 345 (2001).

[37] D. M. Zuckerman and E. Lyman, J. Chem. Theory Comput. **2**, 1200 (2006).

[38] Y. M. Rhee and V. S. Pande, Biophys. J. **84**, 775 (2003).

[39] M. M. Seibert, A. Patriksson, B. Hess, and D. van der Spoel, J. Mol. Biol. **354**, 173 (2005).

[40] H. Fukunishi, O. Watanabe, and S. Takada, J. Chem. Phys. **116**, 9058 (2002).

[41] P. Liu, B. Kim, R. A. Friesner, and B. J. Berne, Proc. Natl. Acad. Sci. U.S.A. **102**, 13749 (2005).

[42] R. Affentranger, I. Tavernelli, and E. E. Di Iorio, J. Chem. Theory Comput. **2**, 217 (2006).

[43] A. Okur, L. Wickstrom, M. Layten, R. Geney, K. Song, V. Hornak, and C. Simmerling, J. Chem. Theory Comput. **2**, 420 (2006).